

## THEORETICAL STUDIES RELATED TO SPALLATION TARGET PHYSICS

D. Filges, T. Armstrong\*, P. Cloth, R.D. Neef  
M. Kloda, and G. Sterzenbach

Institut für Reaktorentwicklung  
Kernforschungsanlage Jülich GmbH  
Postfach 1913

D-5170 Jülich, Federal Republic of Germany

\*Science Applications, Inc. 1200 Prospect St.  
La Jolla, California, 92037, USA

### 1. Introduction

A calculational program is underway at KFA-IRE to investigate various aspects of the German spallation target station design. The major objectives of these theoretical studies are: (1) To assess expected performance of the present preliminary reference design target. This includes neutronics (e.g., predictions of neutron output spectra for continuous, pulsed, and hybrid operation); heating, and cooling requirements; radiation safety aspects (activation, shielding requirements, potential environmental hazards, etc.); and radiation damage levels for materials. (2) To investigate the effects, and possible design improvements, due to various parameter variations (target material alternatives, such as lead vs. uranium, moderator-reflector materials and arrangements, etc.); and, (3) to ascertain the accuracy of the theoretical models being used for such predictions, which includes performing benchmark physics experiments for simple target-moderator configurations.

The basic calculational methods and computer codes being used are summarized in Section 2, and the nature of several experiments that have been performed for code validation purposes are briefly discussed in Section 3. The main emphasis of our work at present is calculations related to evaluation of the preliminary target station design. These calculations are still in progress, but some interim results are presented in Section 4.

### 2. Calculational Methods

The main computer codes being used are the Monte Carlo codes HETC, for high-energy particle transport, and MORSE, for low-energy ( $\leq 15$  MeV) neutron and gamma-ray transport. The version of HETC operating at KFA has been interfaced with a combinatorial geometry module, so it is possible to use the same geometry description input for both HETC and MORSE.

A rather general HETC analysis code, called SIMPEL, has been written to compute, for example, flux and current spectra (over volumes or across surfaces), energy deposition, and residual nuclei distributions. One feature of SIMPEL is that a combinatorial geometry description can be input to define regions for computing spatial distributions within the material volumes used in the HETC calculation. Thus, analyses for different spatial grids can be performed without having to perform additional transport calculations.

For the MORSE calculations, two sets of cross sections have been used: (1) the coupled neutron/gamma-ray EPR Library, containing 100 neutron groups (one thermal group) and 21 gamma-ray groups and (2) a 53-group neutron set (26 groups below 1-ev, including up-scattering), generated from ENDF/B-IV using the KFA version of the code system RSYST. The EPR Library has been used mainly for energy deposition calculations. For MORSE energy deposition calculations, kerma-factors generated by the MACK code and cross section library were used.

### 3. Experiments for Model Validation

Several experiments have been performed at the SIN (600 MeV proton beam) and SACLAY (at 600 and 1100 MeV) accelerators to measure, by activation techniques, the neutron flux produced by proton bombardment of bare and moderated thick targets. Target materials of Pb, Pb-Bi, and depleted U and H<sub>2</sub>O and D<sub>2</sub>O moderators have been considered. For the bare target measurements, rhodium foils were used (threshold  $\approx 0.1$  MeV) the thermal flux inside the moderators was measured using dysprosium

foils. Most of the data from these measurements have not yet been fully analyzed, and only preliminary experimental/theoretical comparisons have been made to date. For example, Fig. 1 shows the dysprosium reaction rate in a large H<sub>2</sub>O moderator surrounding a cylindrical (15 cm dia x 60 cm long) Pb-Bi target bombarded by 590-MeV protons. The results are given as a function of radial distance from the target surface in a plane 10 cm from the front of the target. The values shown are calculated reaction rates, and, while the magnitude of the measured curve has been normalized to the calculation, the shapes of the two distributions are in rather good agreement. The peak radial reaction rate in Fig. 1 corresponds to a calculated thermal flux of about  $1.6 \times 10^{-2} \text{ n.cm}^{-2} \text{ s}^{-1}$  per incident proton per second.

#### 4. Theoretical predictions for reference design target

##### 4.1 Configuration

A three-dimensional simulation of the target station configuration shown in Figure 2 has been used for initial radiation transport calculations. It should be emphasized that this model is for initial calculations only and based on preliminary design considerations; calculations for variations toward optimization have not yet been made, although several modifications for improved performance are believed possible.

The design of Fig. 2 is of a "hybrid" type, with a D<sub>2</sub>O moderator and "cold source" above the rotating target (for high continuous flux) and a fast moderator with reflector below the target (for high peak flux). The target region where most of the proton interactions take place consists of lead rods with aluminum cladding and water coolant. A homogeneous mixture of these constituents is used in the calculations.

Proton beam parameters assumed are: 1100 MeV, gaussian beam profile (FWHM = 4 cm), 5 mA average current, and 100 milliamperes peak current.

##### 4.2 Neutronics

The spatial distribution of the low-energy ( $\leq 15$  MeV) neutron leakage current from the target wheel surface is shown in Fig. 3. A total of  $29.4 \text{ n/p} \leq 15$  MeV are produced, and the target wheel yield (neutron escapes without surrounding materials) is  $25.3 \text{ n/p} \leq 15$  MeV and  $1.8 \text{ n/p} > 15$  MeV. The total neutron leakage from the target with surrounding materials (i.e., the integral of the curves of Fig. 3 over the target wheel surface, which includes neutrons that reflect back into the target and subsequently escape) is  $69.5 \text{ n/p}$ .

The neutron flux as a function of vertical distance in the D<sub>2</sub>O tank (averaged over 20 cm diameter volume about the tank axis) is shown in Figure 4. (These calculations were made without the cold source, or beam tubes, in the D<sub>2</sub>O tank.) The flux values shown have been normalized for an average beam current of 5 mA. The maximum thermal flux in the D<sub>2</sub>O is  $\bar{\phi}_{th} = 7 \times 10^{14} \text{ n/cm}^2\text{-s}$  and occurs at a height of about 15 cm, which is the location where the cold source would be placed.

For the H<sub>2</sub>O moderator, we calculate an omnidirectional thermal flux of  $6.6 \times 10^{-3} \text{ n.cm}^{-2}\text{s}^{-1}$  per p ( $\pm 15$  % statistical error, one standard deviation) just outside the moderator (i.e., in a "detector volume" 0.5 cm thick placed in the void adjacent to the exit face of the moderator). For a peak current of  $\bar{I}=100$  mA, this corresponds to a peak thermal flux of  $\bar{\phi}_{th} = 4.1 \times 10^{15} \text{ n/cm}^2 \text{ sec}$ , which is near (approximately within statistics) the nominal design objective of  $5.5 \times 10^{15} \text{ n/cm}^2 \text{ s}$ . (It should be noted that this calculated value is for a "solid" moderator. Under certain conditions, the thermal neutron output can be enhanced if there are "holes" near the surfaces; e.g., some measurements have shown a factor of two increase.)

The above flux values for both the D<sub>2</sub>O and H<sub>2</sub>O moderators are in agreement with measurements for similar configurations, as reported by G. Bauer in a separate paper.

#### 4.3 Heating Calculations

The energy deposited in various components of the target station has been calculated to indicate general cooling requirements (Table 1). The energy deposited in the target is equivalent to about 50 % of the incident beam energy, with about 25 % to all other components and 25 % into binding energies associated with secondary particle production.

We have also computed the heating expected from the decay of radionuclides produced in the target should coolant flow be interrupted and the beam shut off. We calculate a maximum value for this "afterheat" with respect to irradiation conditions (infinite operating time, immediately after shutdown) to be about 38 kilowatts (compared to 2.9 megawatts during operation, Table 1) and a spatially maximum specific heating inside the target of only  $\sim 1$  watt/cm<sup>3</sup>. Thus, this afterheat is not expected to be a problem should loss of coolant occur.

The calculated energy deposition inside the target (as a function of depth in the beam direction in various radial intervals about the beam axis) is shown in Figure 5. The spatially maximum deposition is about 1.2 MeV/cm<sup>3</sup> per incident proton, which, for a peak current of 100 mA, corresponds to a deposition rate of 120 kilowatts/cm<sup>3</sup> during the pulse.

#### 4.4 Activation

Fig. 6 shows the residual nuclei distributions, calculated using HETC, from spallation collisions with the lead in the target. We find the total radionuclide production inside the target from Pb, O and Al spallations to be about 2.7 radionuclides per incident proton, corresponding to saturation activity (for 5 milliamperes average current) of 2.3 megacuries. Most of this activation is from interactions with the lead; for example, the saturation coolant water activity is 44.6 kilocuries.

In addition to spallation, radioactive products can be generated by high-energy fission interactions with the lead. For the cal-

culated neutron and proton flux spectra over the target volume, the fission cross section is about 3.5 % of the spallation cross section, so fission is expected to contribute only about 7 % of the residual nuclei from lead, with fission product masses peaked at  $A \sim 90$ .

#### 5. Further calculations planned

The main theoretical work planned for the near future includes: (1) completion of calculations to assess the neutronics of the reference design configuration, including time dependence of the neutron output and neutron spectra produced by the cold source; (2) effects of different moderator materials (e.g., lead) and different target material (i.e., uranium); (3) calculations related to target station shielding and radiation safety; and (4) further experimental data analysis and theoretical comparisons for model validation.

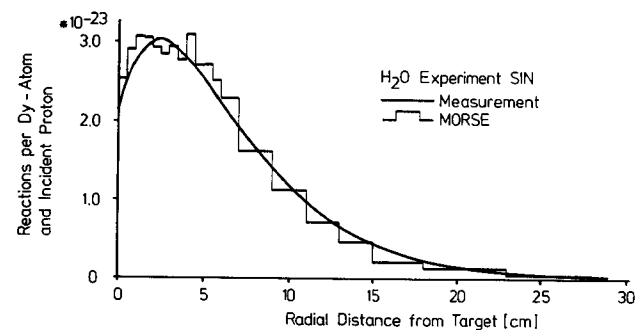


Fig. 1: Experimental/Theoretical Comparison for Neutron Reaction Rate in H<sub>2</sub>O, 590-MeV Proton Bombardment of Pb-Bi Target.

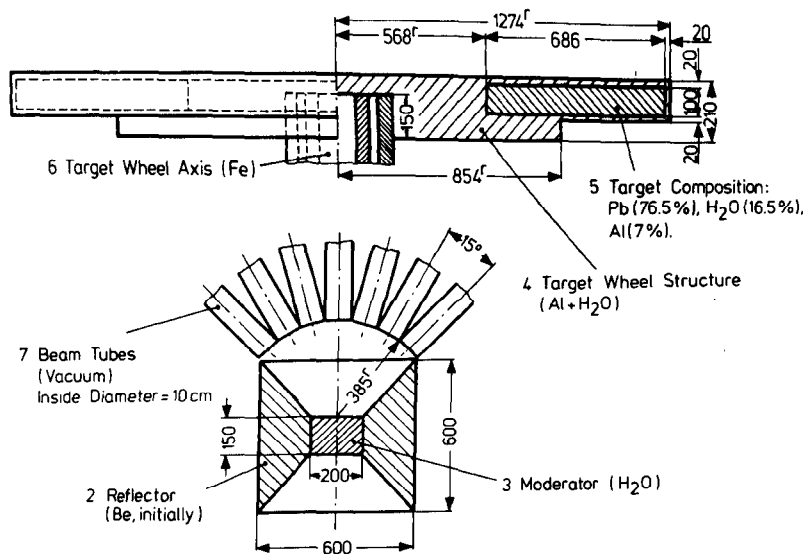


Fig. 2: Target Configuration Used for Calculations

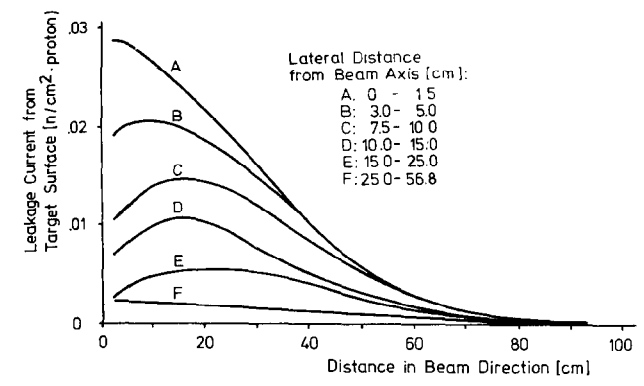


Fig. 3: Neutron Leakage from Target Wheel

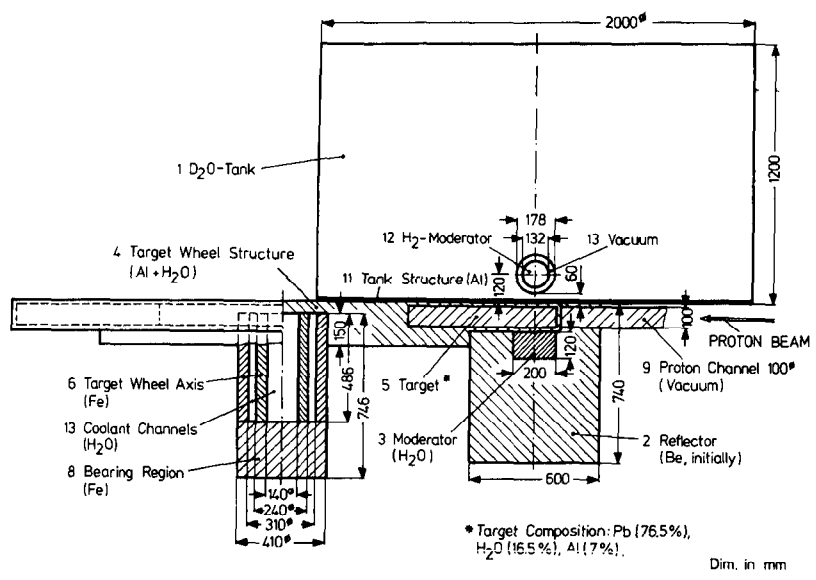


Fig. 2: Target Configuration Used for Calculations

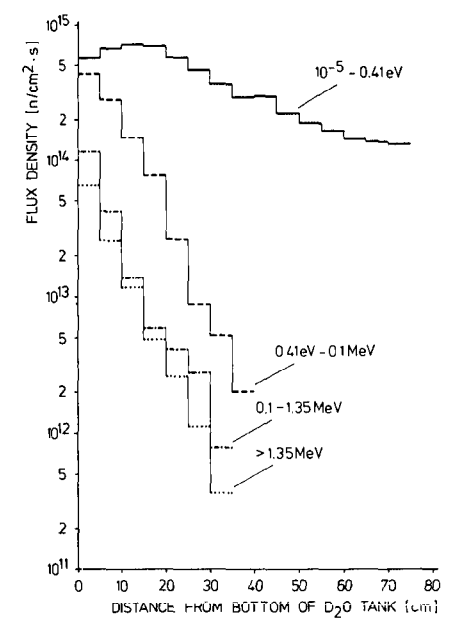


Fig. 4: Neutron Flux Distribution in D<sub>2</sub>O Tank

TABLE 1 ENERGY DEPOSITION IN VARIOUS REGIONS OF TARGET STATION

Region Number (a)	Region Description	Material	ENERGY DEPOSITION		
			MeV per incident proton	Per cent of beam energy	Deposition rate (kilowatts) (c)
5	Target	Pb(76,5%), H <sub>2</sub> O(16,5%),Al(7%)	571.0	51.9	2,854
(b)	Shield	Fe	81.8	7.4	407
4	Wheel: Structure	Al(92%),H <sub>2</sub> O(8%)	61.9	5.6	308
1	Heavy Water	D <sub>2</sub> O	58.3	5.3	292
2	Reflector	Be	29.1	2.6	143
11	D <sub>2</sub> O Tank Bottom	Al	13.9	1.3	72
3	Moderator	H <sub>2</sub> O	3.5	0.3	16
6	Wheel: Axis	Fe	1.6	0.15	8
12	Cold Source	H <sub>2</sub>	0.5	0.05	3
13	Wheel: Coolant Channel	H <sub>2</sub> O	0.3	0.03	2
8	Wheel: Bottom	Fe	~0.2	~0.02	~1
Total Deposition:			822.1	74.8	4,106
Nuclear Binding Energy (Inferred):			277.9	25.2	1,394
			1100.0	100.0	5,500

(a) See Figure 2  
 (b) Shield is assumed to completely surround target station  
 (c) For 5 milliamperes average current, 1100 MeV proton beam

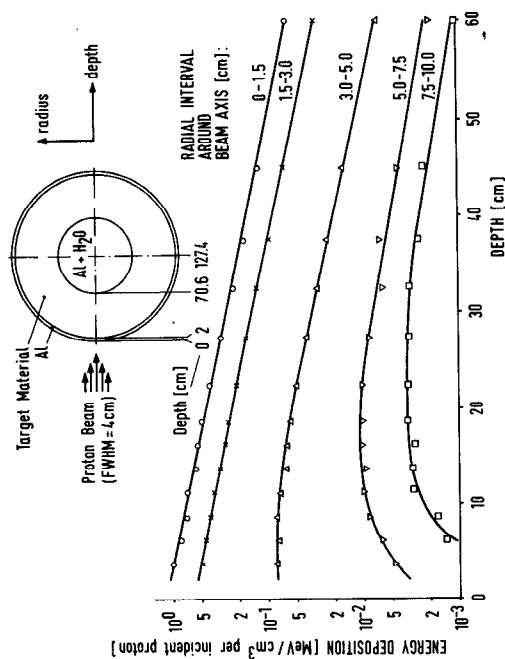


Fig. 5: Energy Deposition Inside Target Wheel

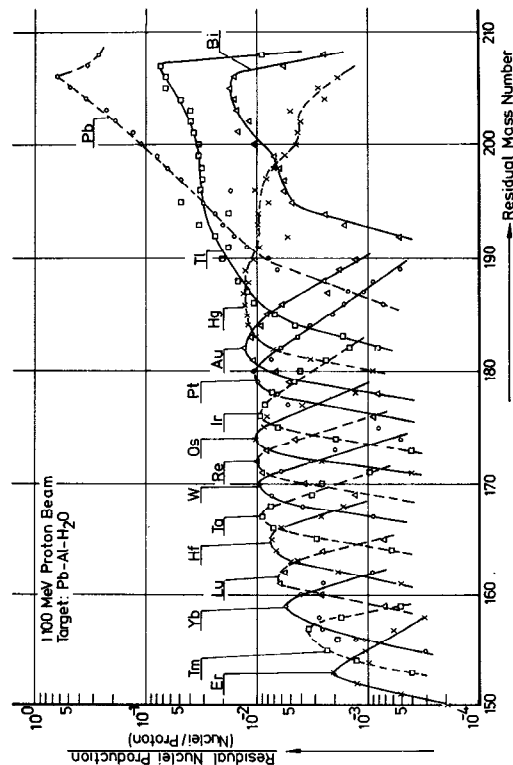


Fig. 6: Spallation Products from Lead in Target